Available online at www.sciencedirect.com
ScienceDirect
Catalysis Today 127 (2007) 31–43
CATALYSIS TODAY
www.elsevier.com/locate/cattod

Five-lump kinetic model with selective catalyst deactivation for the prediction of the product selectivity in the fluid catalytic cracking process

G.M. Bollas *, A.A. Lappas, D.K. Iatridis, I.A. Vasalos

Chemical Process Engineering Research Institute (CPERI), Centre for Research and Technology Hellas (CERTH), PO Box 361, 57001 Thermi-Thessaloniki, Greece

Available online 9 April 2007

Abstract

The effective simulation of the fluid catalytic cracking (FCC) operation requires a good understanding of many factors such as, reaction kinetics, fluid dynamics, and feed and catalyst effects. The different product slates that can be obtained are the consequence of a complex reaction scheme including cracking, isomerization, hydrogen transfer, oligomerization, etc. Furthermore, the catalyst deactivation may affect each one of the reactions in different ways, which creates an additional reason for different variation with time-on-stream of the yield to each product. On the basis of the experimental data of the FCC pilot plant operated in Chemical Process Engineering Research Institute (CPERI, Thessaloniki, Greece), a lumping model was developed for the prediction of the FCC product distribution. The lumped reaction network involved five general lumps (gas oil, gasoline, coke, liquefied product gas, and dry gas) to simulate the cracking reactions and to predict the gas oil conversion and the product distribution. The paths of catalyst deactivation were studied and a selective deactivation model was adopted that enhances the fundamentality and accuracy of the lumping scheme. The hypothesis of selective catalyst deactivation was found to improve the product slates prediction. Models with different assumptions were examined, regarding the behavior of the catalyst, as deactivated, and its effect on the reactions of the lumping scheme. A large database of experiments, performed in the FCC pilot plant of CPERI was used to verify the performance of the models in steady state unit operation. The simulation results depict the importance of incorporating selective catalyst deactivation functions in FCC lumping models.

Keywords: Fluid catalytic cracking; Lumping model; Selective catalyst deactivation; FCC product distribution

1. Introduction

The fluid catalytic cracking (FCC) unit is the workhorse of modern refineries for the production of valuable transportation fuels such as gasoline and diesel, as well as the source of raw materials for important downstream processes that also contribute to the gasoline pool. New world trends in product demands to meet more severe legislation about fuel compositions, raise the significance of controlling the FCC product selectivity. The different product slates of the FCC process are the consequence of the complex interplay between reactions such as cracking, isomerization, hydrogen transfer, oligomerization, etc. The complexity of gas oil mixtures, which are the typical FCC feeds, makes it extremely difficult to characterize and describe the inherent kinetics at a molecular level. Hence, one is forced to examine generalities rather then details. One of the methods used to do this is to consider the behavior of groups of compounds as a unit. In this way similar components are grouped into a few ''cuts'' or ''lumps''. Therefore, the study of the reactions involved in the catalytic cracking process has followed the lumping methodology.

The number of lumps of the proposed models for catalytic cracking reactions has been consecutively increasing to obtain a more detailed prediction of product distribution. In the first kinetic model (3-lump), proposed by Weekman [1], reactants and products were lumped into three major groups: gas oil, gasoline, and light gas plus coke. Yen et al. [2] and Lee et al. [3]

* Corresponding author at: Chemical Process Engineering Research Institute, Centre for Research and Technology Hellas, 6th km. Charilaou – Thermi Rd., PO Box 361, Thessaloniki GR-57001, Greece. Tel.: +30 2310 498305; fax: +30 2310 498380.
E-mail address: gbollas@cperi.certh.gr (G.M. Bollas).

0920-5861/$ – see front matter © 2007 Elsevier B.V. All rights reserved.
doi:10.1016/j.cattod.2007.02.037

took one step forward by dividing the light gas plus coke lump into two different lumps C_1–C_4 gas and coke, developing the first 4-lump models for fluid catalytic cracking. Advancing the lumping methodology, Corella and Frances [4] developed a 5-lump model, in which the gas-oil lump was divided into its heavy and light fractions. Dupain et al. [5] simplified the 5-lump model of Corella and Frances [4] for the specific case of the catalytic cracking of aromatic gas oil, by reducing the reactions involved in the lumping scheme. Another 5-lump model was developed by Larocca et al. [6], in which the 3-lump model of Weekman was modified by splitting the gas oil lump into aromatic, paraffinic, and naphthtenic lumps. Ancheyta-Juarez et al. [7] followed a different approach in their 5-lump models development, in which they considered the gas oil as one lump, but divided the gas lump into two lumps (liquefied product gas and dry gas). 6-Lump models were developed by Takatsuka et al. [8] (including the resid as a separate lump to predict the catalytic cracking of residual oil), and Oliveira and Biscaia [9] (emphasizing in the catalytic cracking of gasoline and paraffinic gas oils). Hagelberg et al. [10] expanded the 5-lump model of Ancheyta-Juarez et al. [7] to an 8-lump model by dividing the gasoline fraction into paraffins, olefins, naphthenes and aromatics. Wojciechowski and Corma [11] proposed a 12-lump reaction scheme for catalytic cracking in which the gas composition was considered in detail. The more advanced model was proposed by Jacob et al. [12], which included 10 lumps (light and heavy gas oil paraffinic, naphthenic and aromatic rings and substituents). On the basis of the 10-lump model of Jacob et al. [12], Ellis et al. [13] developed a more advanced model capable of predicting the light gas product slate, using empirical algebraic equations.

One additional important issue that varies in the approaches mentioned, is the model equation that describes the catalyst deactivation. During reaction, the cracking catalyst deactivates due to the formation and deposition of coke, which severely affects the catalyst performance. The catalyst decay phenomenon is commonly quantified using empirical functions of the time-on-stream concept of Voorhies [14]. In most cases, the catalyst decay is modeled with an exponential or a power function. The exponential function, widely referred as first-order decay model [15], describes well the decay behavior of the catalyst for times-on-stream higher then 40 s [15] or 1 min [6]. However, for small times-on-stream, which is the case for typical commercial FCC risers and FCC pilot plants with residence times lower than 10 s, the power function suits better the experimental data [15]. The background theory for this behavior is that as deactivated the catalyst behaves different. Corella and Asua [16,17] developed a rigorous and general model to describe the kinetics of catalyst deactivation with no restrictions on time-on-stream. With the assumption of ''homogeneous catalyst surface'', which means that all of the catalyst active sites have the same strength, as deactivation by coke proceeds in parallel series, they were able to fit experimental data from both commercial and laboratory units to their general decay model [15]. The general conclusion of the above researchers was, that for effective simulation of commercial FCC risers only experimental data obtained at times below approximately 10–20 s are useful.

It is well known that the coke deposition on the catalyst surface affects not only its activity (affecting the conversion of the reactants), but also its selectivity (affecting the product distribution) [18]. That is, the deactivation of the catalyst may affect each one of the reactions in a reaction network (a lumping scheme in the case of FCC modeling) in different ways. This difference in the variation with time-on-stream of the yield to each product, owed to catalyst deactivation, can be modeled with a *selective deactivation* kinetic model. The kinetic expressions in such a model involve a different decay exponent in each one of the deactivation functions that are multiplied to the respective reaction kinetic constant. In other words, it is assumed that the catalyst deactivation affects each reaction in a different way or extent. However, due to the overparameterization that selective deactivation models introduce to the estimation procedure of the kinetic constants, usually *non-selective deactivation* models are applied in which the deactivation of catalyst is assumed to affect in the same way all the cracking reactions.

On the basis of the experience earned in the past years by the aforementioned researchers, a lumped reaction network was drawn for the simulation of the experimental data of the FCC pilot plant operated in Chemical Process Engineering Research Institute (CPERI). The kinetic scheme involved five general lumps, namely the gas oil, the gasoline, the coke, the liquefied product gas (LPG), and the dry gas, while selective deactivation models were applied, as to enhance the fundamentality and accuracy of the model. In order to avoid overparameterization of the mathematical problem four different simplifying assumptions were examined regarding the way catalyst deactivation affects the cracking reactions: (a) in the same way for all reactions, (b) differently for each different reactant of the lumping scheme, (c) differently for each product of the lumping scheme, and (d) via thermal cracking dry gas production (not affected by catalyst deactivation). The results of each model were compared to each other on the basis of statistical indicators. Emphasis was given to exploring the results of selective catalyst deactivation models, as this type of models is expected to enhance the fundamentality of the lumped scheme.

2. Experimental setup

The FCC pilot plant of CPERI (Fig. 1) operates in a fully circulating mode and consists of a riser reactor with 7 mm i.d., a fluid bed regenerator, a stripper and a lift line [19]. In the riser the cracking reactions take place and at the riser exit the mixture enters the stripper vessel for the separation (stripping) of gas from catalyst. The reaction product, from the stripper exit, flows through a heat exchanger for the condensation of heavier compounds. Thereupon, the mixture is led to a stabilizer column for complete separation of the liquid and gaseous products. The mixture of gasoline, light cycle oil (LCO) and heavy cycle oil (HCO) is obtained through the bottom of the stabilizer. The yield to liquid products is measured with the ASTM simulation distillation method. The fluid bed regenerator is used to burn-off the carbon, deposited

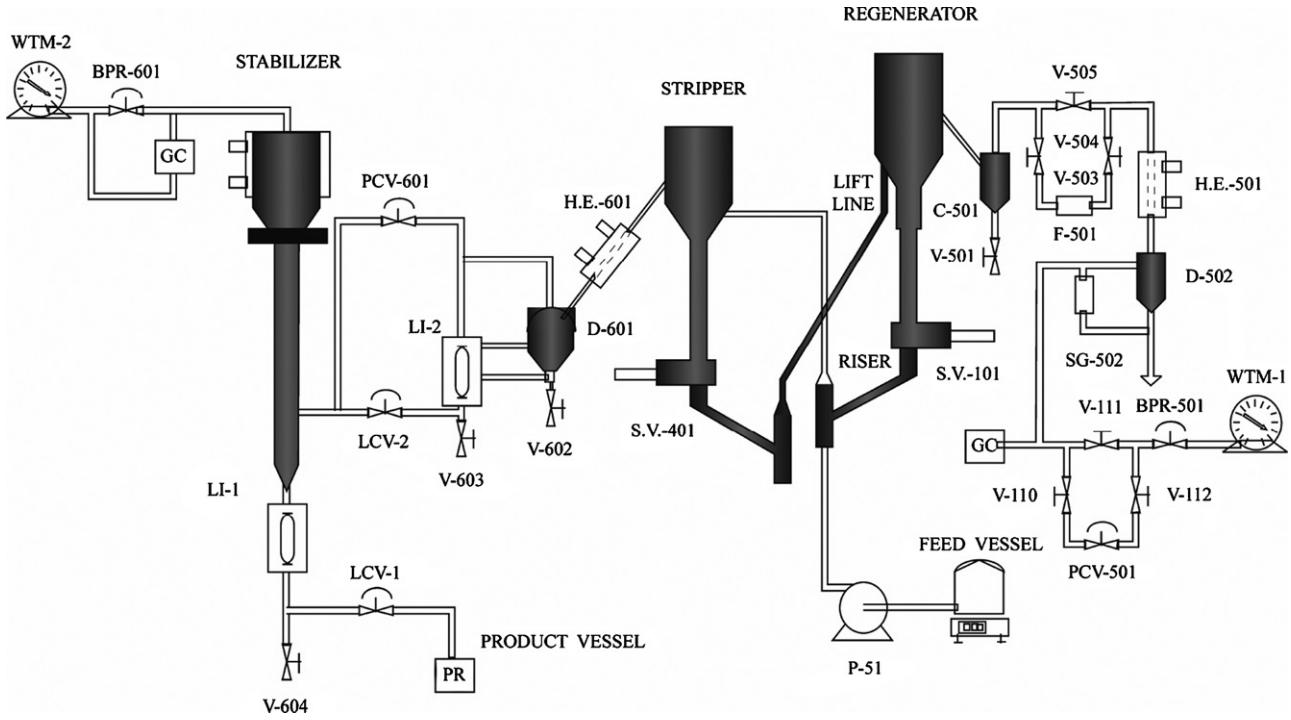

Fig. 1. Schematic diagram of the FCC pilot plant of CPERI.

on the catalyst surface as a by-product of the cracking process. Two wet test meters and two gas chromatographers determine the volumetric flow rates and the composition of the fuel and cracked gas, respectively. An on-line oxygen analyzer always monitors the excess of oxygen to obtain good catalyst regeneration. Pseudo-isothermal riser and adiabatic regenerator operating profiles are established with the use of electrical heaters that control the temperature along their height.

The operation of the pilot unit provides the ability to examine the process under steady feed and/or catalyst properties, in order to isolate their respective effects on cracking and develop property-oriented correlations for each subset of process variables. The lumping scheme and the deactivation profiles, discussed in this paper, were developed on the basis of 38 pilot experiments performed with constant feed and catalyst, while varying the unit operating conditions to result in catalyst residence times in the range of 3–18 s. The experiments were performed at two temperatures 520 and 560 °C, to provide an estimate of the reactions activation energies. Moreover, experiments were performed at three different gas-oil feed rates (10, 51 and 18 g/min) to examine the effect of gas-oil and catalyst residence time on the product slate. The feedstock and catalyst properties used for this experimental series are presented in Table 1.

3. Model development

The kinetic model used in this study was a five-lump model, in which the reactant-products mixture was divided into five groups according to their carbon number and boiling point ranges. The five lumps were the gas oil (with TBP in the range of 170–510 °C), the gasoline (C_5—221 °C), the liquefied product gas (C_3–C_4), the dry gas (C_1–C_2, H_2, and H_2S) and the coke. These five groups were incorporated in the reaction network of Fig. 2. The reactions involved in the reaction network are described by Eqs. (1)–(5), where y_1 is the molar

Table 1
Bulk properties of the feedstock and the catalyst used in the experiments examined

Feedstock properties	
Gravity (API)	25.2
Refractive index (at 20 °C)	1.5016
Sulfur (wt%)	1.82
Nitrogen (wt%)	0.096
Carbon (wt%)	85.4
Con. carbon residue (wt%)	0.07
TBP distillation (°C)	
IBP	170.3
10%	318.6
30%	385.5
50%	425.2
70%	452.9
90%	485.4
FBP	509.4
Catalyst properties	
Bulk density (kg/m^3)	840
Mean particle diameter (μ)	80
Surface area (m^2/g)	158
Unit cell size (Å)	24.26
Al_2O_3 (wt%)	39.1
Re_2O_3 (wt%)	0.65
Fe (wt%)	0.59
Ni (ppm)	163
V (ppm)	362
Sb (ppm)	<50
MAT	70

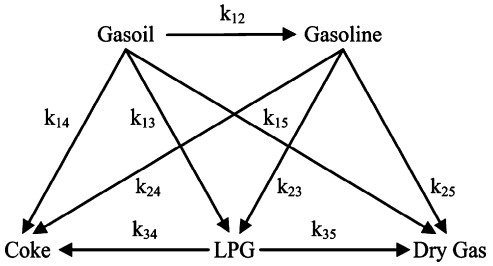

Fig. 2. Schematic diagram of the five-lump model examined.

concentration of gas oil, y_2 of gasoline, y_3 of LPG, y_4 of coke, y_5 of dry gas, while τ is the space time in the riser reactor. The pilot reactor was simulated as a pseudo-isothermal plug flow rector. Each pair of k_{ij} and ϕ_{ij} represents the kinetic constant and the catalyst activity of the reaction of lump i to j, respectively. The factors v_{ij} are the ratios of the molecular weight of lump i over lump j and are used as stoichiometric coefficients for the reaction of lump i to j, in order to satisfy the global mass balance. The cracking reactions of gas oil to products were assumed of second order kinetics. The apparent gas oil kinetics are higher than first order, because of the existence of many different compounds with different reaction rates that cause a faster depletion of the reacting species. As a result, the reaction rate slows faster with conversion compared to the case of a single compound [20]. For the cracking of gasoline and LPG first order kinetics are generally accepted [4,7,10,11,21].

$$\frac{dy_1}{d\tau} = -(k_{12}\phi_{12} + k_{13}\phi_{13} + k_{14}\phi_{14} + k_{15}\phi_{15})y_1^2 \quad (1)$$

$$\frac{dy_2}{d\tau} = v_{12}k_{12}\phi_{12}y_1^2 - (k_{23}\phi_{23} + k_{24}\phi_{24} + k_{25}\phi_{25})y_2 \quad (2)$$

$$\frac{dy_3}{d\tau} = v_{13}k_{13}\phi_{13}y_1^2 + v_{23}k_{23}\phi_{23}y_2 - (k_{34}\phi_{34} + k_{35}\phi_{35})y_3 \quad (3)$$

$$\frac{dy_4}{d\tau} = v_{14}k_{14}\phi_{14}y_1^2 + v_{24}k_{24}\phi_{24}y_2 + v_{34}k_{34}\phi_{34}y_3 \quad (4)$$

$$\frac{dy_5}{d\tau} = v_{15}k_{15}\phi_{15}y_1^2 + v_{25}k_{25}\phi_{25}y_2 + v_{35}k_{35}\phi_{35}y_3 \quad (5)$$

It should be noted that Eq. (5) holds for the forming of catalytic coke as a by-product of the catalytic reactions. In addition to catalytic coke, a small portion of coke is supposed to be formed as thermal and contaminant coke. For the specific feedstock studied (Table 1) the yield of the non-catalytic coke was estimated 0.68 wt% [22]. This amount of coke is assumed to form instantly, and is used as initial value for y_4, whereas it is subtracted from the initial concentration of y_1, for the solution of the system of differential equations (1)–(5). More details on the coke types and the way they were predicted for a number of feedstocks examined in CPERI can be found elsewhere [22].

The catalyst activity is calculated as a function of the catalyst residence time (t_c) by Eq. (6).

$$\phi_{ij} = t_c^{-n_{ij}} \quad (6)$$

If a *non-selective catalyst deactivation* is assumed then all the catalyst deactivation exponents n_{ij} should be equal (leading to one catalyst deactivation exponent n). Another scenario is to assume the cracking of each reactant (gas oil, gasoline, LPG) to be characterized by a constant catalyst decay exponent (which leads to three catalyst deactivation exponents n_{1j}, n_{2j}, n_{3j}). This assumption is correct if one considers uniform catalyst surface (all active sites of the catalyst having the same strength) and that blocking the catalyst pores due to coke formation is the dominant catalyst deactivation effect on reactivity. In this case diffusion phenomena are important and the average molecular size of each reactant plays a dominant role on how deactivated the catalyst appears to it. The above phenomenon will be referred in this paper as *reactant oriented catalyst deactivation*. A third hypothetical scenario is that the products characterize the catalyst activity level in each of Eqs. (1)–(5), which leads to four catalyst deactivation exponents n_{i2}, n_{i3}, n_{i4}, n_{i5}. This can be attributed to the fact that different active sites are used for each one of the reactions mentioned and the yield of each reaction is dependent on the strength of the site used. Furthermore, diffusion phenomena as caging of large hydrocarbon molecules in the catalyst pores by coke deposition, could lead to selective behavior of the catalyst towards the production of light products. In such cases the products characterize the catalyst activity involved in the reactions towards their production. The above phenomenon will be referred in this paper as *product oriented catalyst deactivation*. In all cases, the theoretically correct way to involve selective catalyst deactivation in a lumping scheme is to assume a different deactivation exponent for each reaction, but this will produce a cumbersome regression problem for the estimation of the kinetic parameters in the reaction network. For this reason one of the above simplifications has to be adopted.

Another issue that has to be considered is the cracking reactions that produce dry gas. It is generally accepted that carbocations are the principal agents responsible for catalytic cracking [11]. From this point of view, the production of dry gas is not in agreement with the carbenium ion theory. Nonetheless, usually a 2–5 wt% of C_1 and C_2 appears in the product slate of the FCC process, which has been ascribed to ''less favored'' types of cracking reactions [11]. A part of this product can be ascribed to competitive thermal cracking reactions occurring in the void volume of the riser. The rest of the C_1 and C_2 product can be explained by secondary reactions of the primary products of the catalytic cracking. Moreover, the metals existing in the surface of an equilibrium catalyst (such as nickel and vanadium) are known for their dehydrogenation activity, producing significant amounts of hydrogen in dry gas [7]. If one considers the deactivation of the catalyst that causes pore blocking, another explanation can be given to the production of dry gas. Wojciechowski and Corma [11] discussed the possibility of the diffusion phenomena to cause caging of product molecules in the catalyst pores, which results in the enhancement of secondary reactions and increase the yield to dry gas. Which one of the above effects is the dominant is far from being understood, while the properties of catalyst and feedstock also interact in all phenomena and increase the complexity of the problem.

In the previous paragraphs it was shown that even for the simple case of a five-lump model for the fluid catalytic cracking so many uncertainties exist and so many assumptions have to be made that the problem is far from being simple. If one considers the complexity of the mathematical and statistical aspects of the problem, then it becomes clear that much effort has to be made to add just a light of knowledge to the development of FCC lumping models. On the basis of the experimental data of CPERI four different scenarios were explored, namely non-selective catalyst deactivation, reactant oriented selective catalyst deactivation, product oriented selective catalyst deactivation, and thermal cracking for dry gas production with reactant oriented selective catalyst deactivation model.

3.1. Mathematical and statistical considerations

For all scenarios the pre-exponential factors ($k_{o,ij}$) and the activation energies (E_{ij}) of the kinetic constants ($k_{ij} = k_{o,ij} \exp(-E_{ij}/RT)$ for each reaction, as well as the deactivation exponents n_{ij} were calculated with non-linear regression against the experimental data of the FCC pilot plant of CPERI. The objective function minimized was the sum of squares of the differences between the estimated and the observed molar concentrations of the mixture at the riser outlet. The system of differential equations (Eqs. (1)–(5)) was solved using the Gear's BDF method [23], while for the non-linear regression procedure a modified Levenberg–Marquardt algorithm [23] was applied. The regression algorithm restricted the estimation parameters to be greater than zero, as non-physical sense exists for inverse reaction rates, positive activation energies and positive deactivation exponents. Regarding the regression procedure, a dataset of experiments performed at constant temperature was used to estimate the catalyst decays n_{ij} for each scenario and to obtain the starting values for the kinetic constants of each reaction scheme. The catalyst activity was considered independent of the riser temperature, as it was shown in this and other works [19,24] that temperature has an almost negligible effect on the coke deposition and thus on catalyst deactivation.

All models examined, except for the case of dry gas production via thermal cracking, are submodels of the same general model described in Eqs. (1)–(5), with a different restriction hypothesized for the catalyst decays n_{ij} of each reaction. For each model the goodness of fit was quantified by the sum of squared errors (SS) of the predicted values. The more complicated models were expected to fit better (have lower sum of squares) than the simpler models, as the curve generated by a more complicated equation (one with more variables) has more inflection points (it wiggles more). To decide if a more complicated model fitted significantly better than a simpler one, statistical calculations were performed. The so called F-test was performed to compare fits. The question answered by the F-test is whether this decrease in sum of squares is worth the ''cost'' of the additional variables (loss of degrees of freedom). The F-ratio quantifies the relationship between the relative increase in sum of squares and the relative increase in degrees of freedom. If the simpler model is correct the F-ratio should receive a value near unity. If the ratio is much greater than unity, then either the more complicated model is correct, or the simpler model is correct but random scatter led the more complicated model to fit better. The answer to this latter question is given by a straight comparison of the F-ratio with the upper quantile of Fisher's $\mathcal{F}$ distribution [25]. Whenever the F-ratio exceeds the upper quantile $\mathcal{F}_{0.05}(dF_1 - dF_2, dF_1)$ the conclusion is that the restriction hypothesized should be rejected and that the complicated model is significantly better than simple one.

4. Model application

All four scenarios discussed in the previous paragraphs were compared using the experimental database of CPERI. Table 2 presents the statistical properties of each regression problem. In all cases examined, the reaction of LPG to coke (r_{34}) was found to receive zeroth kinetic constant, which means that this reaction was found to be negligible, at least for the experimental series examined. Hence, the pre-exponential factor and the activation energy of reaction r_{34} were removed from the degrees of freedom analysis shown in Table 2. Table 3 presents synoptically the relative errors in the prediction of the yields to each lump for the cases examined. The results of the cases examined are also presented graphically in Figs. 3–6.

Typically, the selectivity of the FCC products is presented in plots of each product versus conversion. This norm does not apply in the present work. The reason for the latter is that the effect of selective catalyst deactivation is examined, which means that further than the dependence of each product on conversion there is the influence of catalyst (or gas-oil) residence time that should be taken into account and depicted in the plots. This can be done in 3D plots; however, the 3D plots do not clearly present trends. Thus, the following form was selected for presenting graphically the ability of each model to simulate the experimental results. Each plot presents the conventional lumps versus conversion dependence for both the experimental and the modeled results. The plotted data are grouped according to the respective experimental gas-oil feed

Table 2
Regression statistics of the scenarios examined

Case examined	Unknowns	Degrees of freedom	Regression sum of squares
Non-selective catalyst deactivation	8 $k_{o,ij}$ – 8 E_{ij} – 1n_{ij} 17 parameters	21	3.470
Reactant oriented selective catalyst deactivation	8 $k_{o,ij}$ – 8 E_{ij} – 3n_{ij} 19 parameters	19	3.325
Product oriented selective catalyst deactivation	8 $k_{o,ij}$ – 8 E_{ij} – 4n_{ij} 20 parameters	18	2.141
Thermal cracking for dry gas production	8 $k_{o,ij}$ – 8 E_{ij} – 2n_{ij} 18 parameters	20	3.443

Table 3
Relative errors (%) between predicted and experimental yields to each lump for the cases examined

Case examined	Gas oil	Gasoline	LPG	Coke	Dry gas
Non-selective catalyst deactivation	1.73	2.17	4.38	5.51	9.45
Reactant oriented selective catalyst deactivation	1.57	2.15	4.34	5.31	8.96
Product oriented selective catalyst deactivation	1.56	2.10	3.86	4.78	4.63
Thermal cracking for dry gas production	1.65	2.07	4.43	5.30	10.73

rate. As mentioned in Section 2 three distinct feed rates were used in the experiments performed for this study. The feed rate is a strong indicator of the time-on-stream, although it is not the only factor influencing it. However, due to the easiness of grouping the experimental data at each feed rate and in order to be consistent with previous work presented in the literature [19], this grouping was maintained. Using this kind of grouping the additional effect (if any) of residence time in the product selectivity should be evident. Moreover, and to increase the readability of the plots of interest, trend lines of the model predictions were calculated and drawn on the plots. These trend lines present bulkily what the model predictions would be if only the conversion and the distinct feed rates were affecting the product selectivity. To perform this, all the inputs were set to their average values of each subset of experiments with constant feed rate and temperature and the catalyst circulation rate was run through its range. The result of the latter is an estimate of the net dependence of each lump on feed conversion for each subset of experiments (with constant feed rate). Nonetheless, these trend lines are drawn only to guide the reader's eye and are not the actual model predictions, which are depicted by data marks.

4.1. Case 1—non-selective catalyst deactivation

The assumption of non-selective catalyst deactivation leads to a regression problem with 17 parameters to estimate and 21

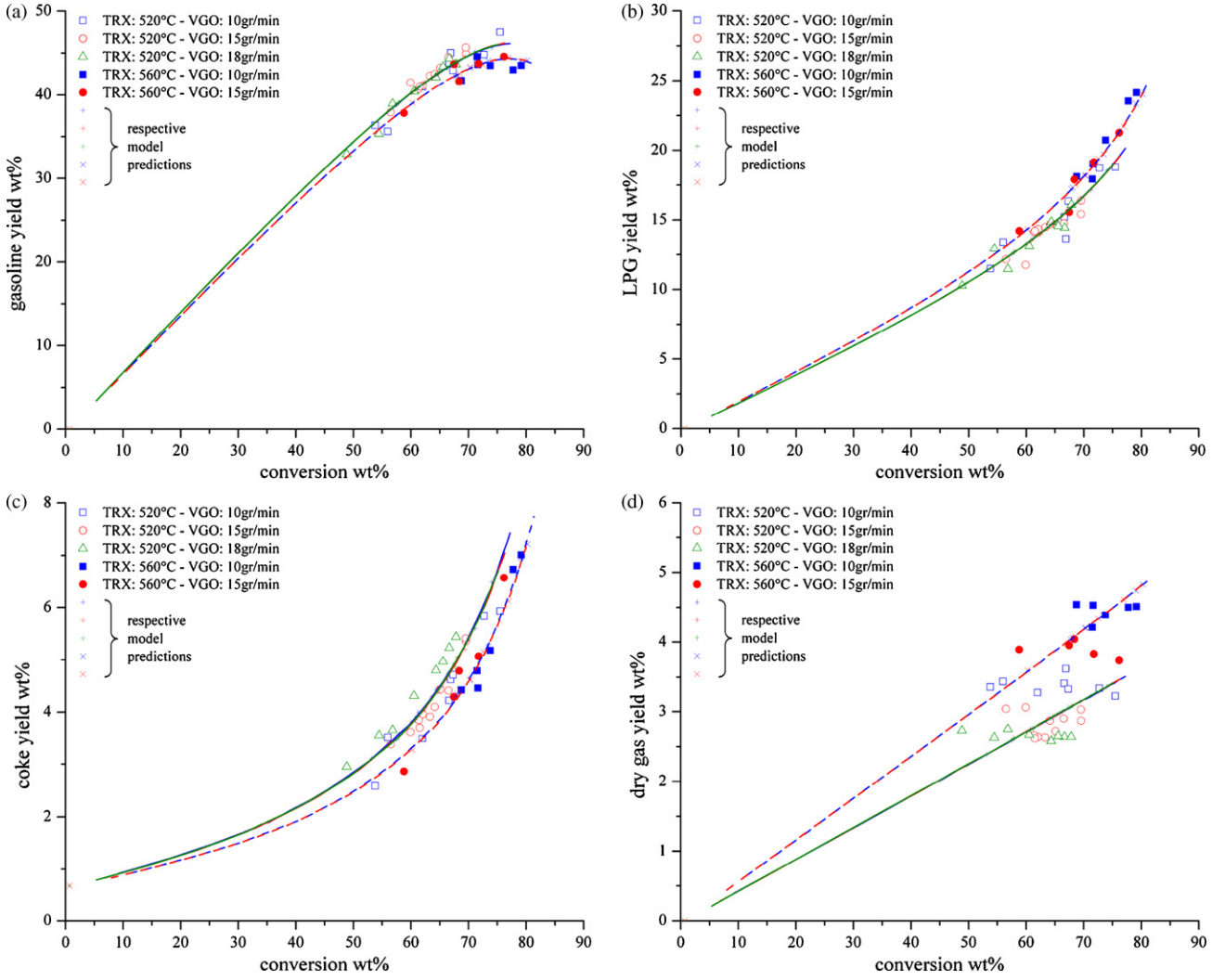

Fig. 3. Product yields wt% vs. conversion wt% modeled (lines) and experimental results (points) for Case 1 (*non-selective catalyst deactivation*): (a) gasoline, (b) LPG, (c) coke, and (d) dry gas.

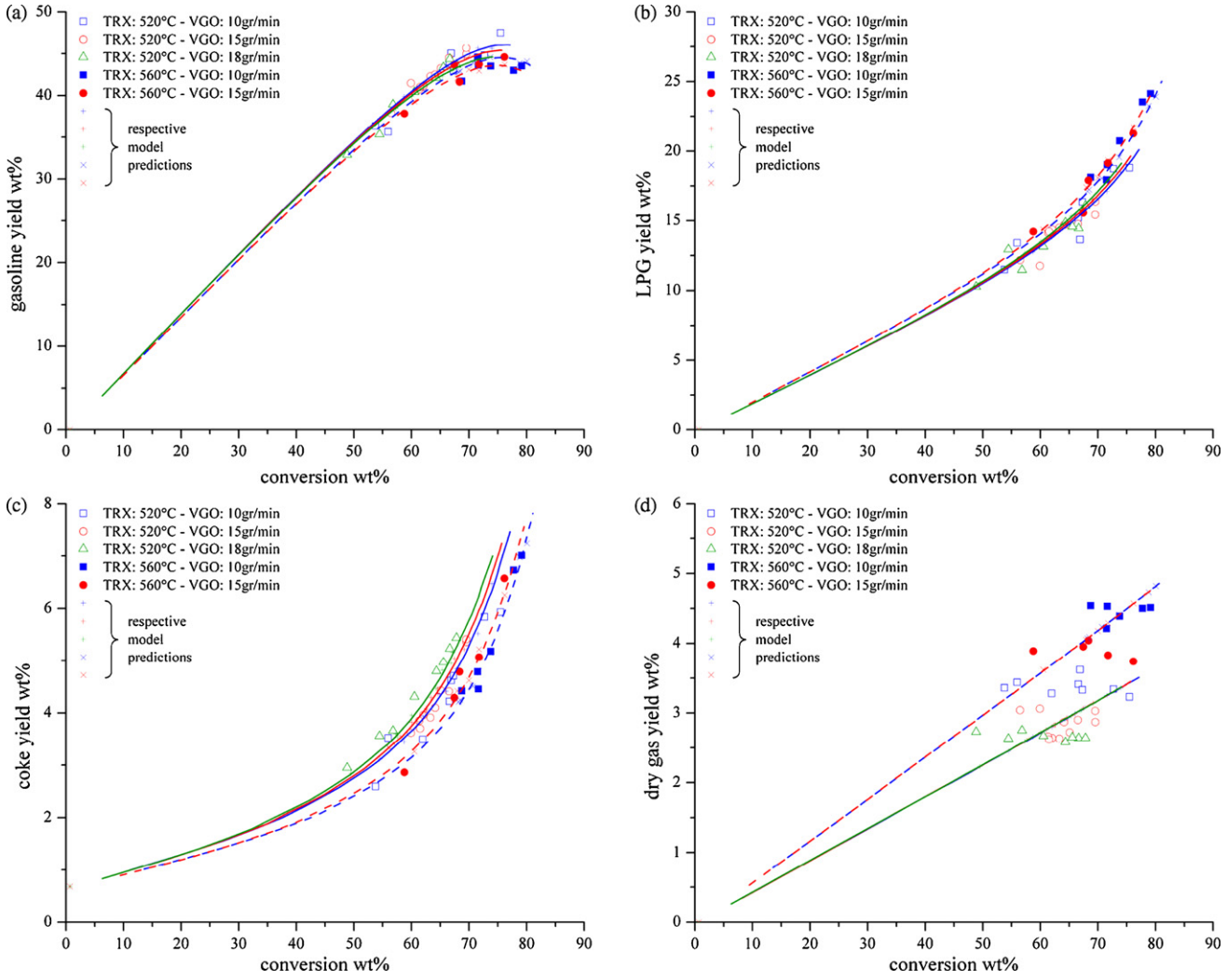

Fig. 4. Product yields wt% vs. conversion wt% modeled (lines) and experimental results (points) for Case 2 (*reactant oriented selective catalyst deactivation*): (a) gasoline, (b) LPG, (c) coke, and (d) dry gas.

degrees of freedom. The statistical properties of this regression problem are shown in Table 2. Table 3 presents the relative errors between the predicted and the experimental yields to each lump, as they are calculated when the regression parameters receive the optimum values shown in Table 4. Generally, the fit appears satisfactory, yet the scatter in the prediction of coke and dry gas is considerable. A visual presentation of the fit is presented in Fig. 3, where the relationship between the experimental and predicted yields wt% to each lump versus conversion wt% is presented. For the case of non-selective catalyst deactivation, when all products are similarly affected by catalyst deactivation, the model responses should appear as polynomial functions of conversion, as proposed by Ancheyta-Juarez and Murillo-Hernandez [26], who developed simple relations of the product yields with the conversion or the time-on-stream. A slight deviation of the model from this rule is evident in Fig. 3 and is owed to the fluctuation of the nitrogen enrichment, used to establish a proper hydrodynamic regime in the bottom section of the pilot riser, which introduces a fluctuation to the initial molar concentration of gas oil. As shown in Fig. 3, the gasoline overcracking, evident at conversions higher than 75–80 wt%, is successfully predicted. The higher temperature (560 °C) promotes the production of light products, as it generally promotes secondary reactions. The activation energies, presented in Table 4, are slightly lower than these usually reported in the literature [1,7,10]. This can be attributed to deviations between the real time operation of the pilot riser and the ideal isothermal operation considered in the models. Another contributing factor to the lower activation energies presented in this work, could be the fact that the experiments examined were performed at only two different temperatures, which limits the evidence of the effect of temperature on the product yields [27].

4.2. Case 2—reactant oriented selective catalyst deactivation

When the catalyst activity of each reaction is supposed to be dominated by the reactants, the regression problem has 19 parameters to estimate and 19 degrees of freedom (Table 2). The optimum values of the parameters of Eqs. (1)–(6) for the

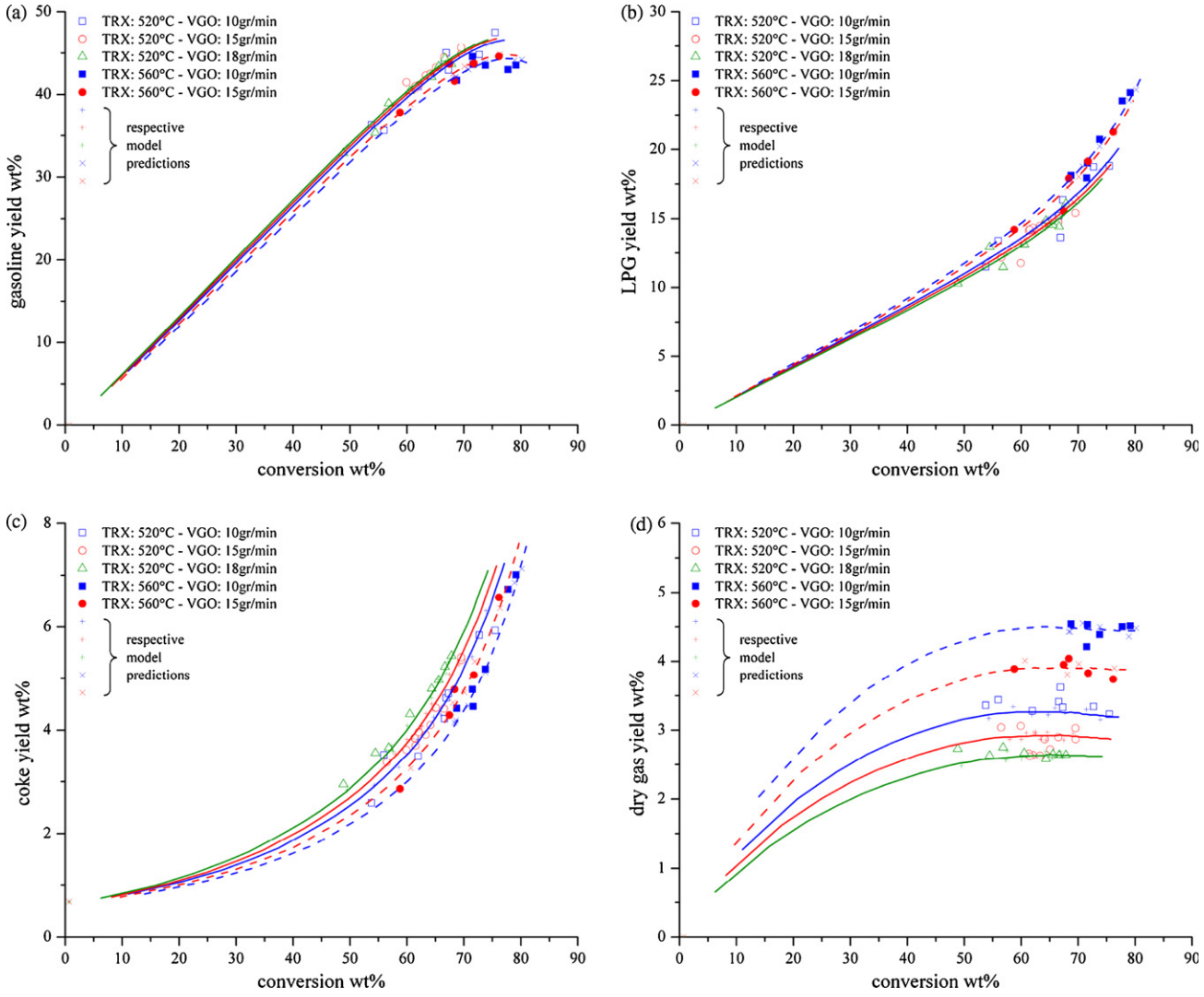

Fig. 5. Product yields wt% vs. conversion wt% modeled (lines) and experimental results (points) for Case 3 (*product oriented selective catalyst deactivation*): (a) gasoline, (b) LPG, (c) coke, and (d) dry gas.

case of reactant oriented selective deactivation are given in Table 4. In Table 3 the relative errors in the prediction of the yield to each lump are presented. The fit for gasoline and LPG is similar to the one of the non-selective catalyst deactivation case, whereas the error in the prediction of conversion, coke and dry gas is reduced. In Fig. 4 the relationship between each lump and conversion is presented. The model predictions (and the trend lines in Fig. 4(a)–(d)) start to dissociate from each other according to the feed rate of each respective subset and follow the observed values. That means that time-on-stream has a different effect on each lump of the lumping scheme, and there is not a straight relationship between the product yields and conversion. In Table 4 a high deactivation exponent is presented for gasoline cracking that almost reaches unity. This observation leads to the conclusion that the catalyst activity for the gasoline reactions to coke, LPG and dry gas drops instantly. Oliveira and Biscaia [9] proposed that gasoline cracking is expected to take place on stronger acid sites, which are deactivated rapidly. The latter implies that catalyst selective behavior is mainly driven by the non-uniformity of the catalyst surface, whilst diffusion phenomena of the reactants molecules are not so significant.

4.3. Case 3—product oriented selective catalyst deactivation

When the catalyst deactivation of each reaction is attributed to the products of this reaction, then 20 parameters are for the regression algorithm to estimate with 18 degrees of freedom (Table 2). The relative errors in the prediction of the yields to each lump are presented in Table 3. The fit for conversion, gasoline, LPG and coke shows a small improvement, while the prediction of dry gas is significantly improved. As shown in Table 4, this major improvement in the prediction of dry gas is owed mainly to the unique deactivation exponent assigned to it, since in this case gas oil, gasoline and LPG contribute to the production of dry gas with reactions affected by a smooth catalyst deactivation profile. Fig. 5 presents the relationship between each lump and conversion. For the case of product oriented selective deactivation the responses of the model (and

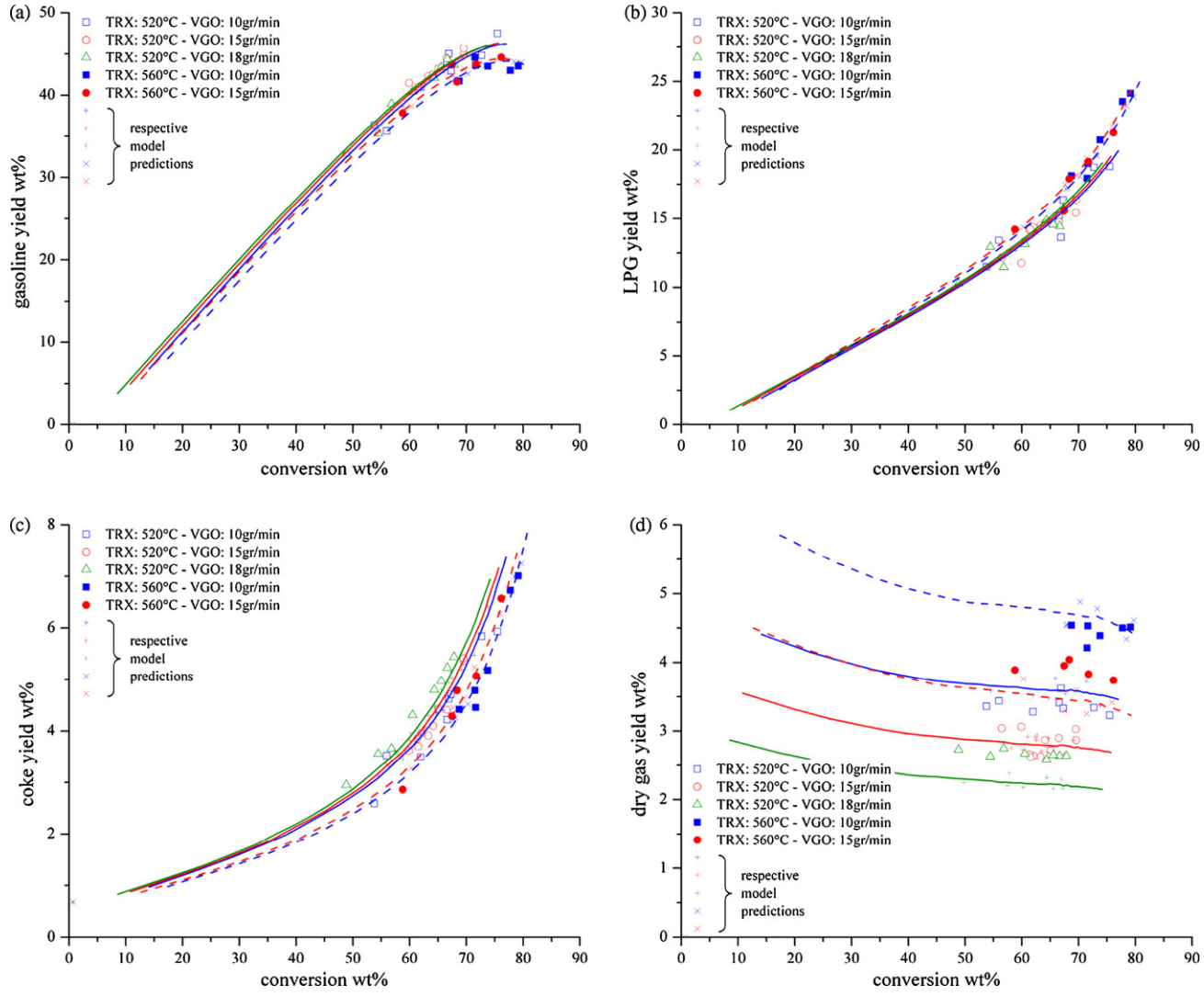

Fig. 6. Product yields wt% vs. conversion wt% modeled (lines) and experimental results (points) for Case 4 (*reactant oriented selective catalyst deactivation with thermal cracking for dry gas production*): (a) gasoline, (b) LPG, (c) coke, and (d) dry gas.

the trend lines in Fig. 5) appear to follow a much different profile than the one of the previous cases. It is evident that the different effect that time-on-stream has on each product-lump of the scheme is described more accurately in this case. The plot of dry gas versus conversion in Fig. 5(d) shows the significant improvement of the product oriented selective deactivation model. The suspicious linear dependence of dry gas on conversion, which was predicted in the previous cases (Figs. 3(d) and 4(d)), is in this case replaced by a theoretically more correct and sensible non-linear one. The reason that the non-selective and reactant oriented selective catalyst deactivation models predicted a linear dependence was that they could not predict the effect of catalyst residence time in dry gas yield. This variation with time-on-stream of the selectivity towards dry gas is successfully predicted by assigning a separate deactivation function to the reactions yielding to dry gas. Moving from reactions yielding coke, to reactions to LPG and finally to reactions to dry gas the catalyst deactivation profile becomes smoother, as it is indicated by the lower catalyst decay exponents in Table 4. It seems that the activity of the reactions towards coke production drops rapidly by the deposition of coke itself, while the reactions towards LPG and dry gas continue at relatively lower catalyst activities and higher times-on-stream. The theory of non-uniform catalyst surface, with different sites being used for the above three different reaction types provides a good explanation to this behavior.

4.4. Case 4—reactant oriented selective catalyst deactivation with thermal cracking for dry gas production

In this case the kinetic scheme is not correctly expressed by Eqs. (1)–(5), since the dry gas production is not a function of the space time τ, but should be expressed as a function of the residence time of the gas phase in the riser. Furthermore, the catalyst deactivation does not affect the reactions towards dry gas production, since dry gas is assumed to be produced via thermal cracking. Hence, the catalyst deactivation functions ϕ_{i5} equal unity. The mathematical formulation of this case results to a regression problem with 18 parameters to estimate and 20 degrees of freedom, as shown in Table 2. The optimum values

Table 4
Estimated parameters for the kinetic expressions of the lumped schemes studied[a]

	r_{12}	r_{13}	r_{14}	r_{15}	r_{23}	r_{24}	r_{25}	r_{34}	r_{35}
Case 1 (*non-selective catalyst deactivation*)									
Pre-exponential factor $k_{o,ij}$	0.07	0.11	0.00014	2.83	22.82	0.00632	31.41	–	31.82
Activation energy E_{ij}	7.46	10.29	2.87	17.70	16.11	3.33	26.77	–	23.60
Kinetic constant k_{ij} (at 520 °C)	2.1E−1	5.7E−2	7.9E−3	1.3E−2	8.5E−4	7.7E−4	1.4E−6	–	1.0E−5
Deactivation constant n_{ij}	0.86								
Case 2 (*reactant oriented selective catalyst deactivation*)									
Pre-exponential factor $k_{o,ij}$	0.07	0.12	0.00021	2.83	22.82	0.00402	31.41	–	31.82
Activation energy E_{ij}	7.11	9.94	2.99	17.34	16.69	3.13	26.94	–	23.54
Kinetic constant k_{ij} (at 520 °C)	2.6E−1	7.4E−2	1.1E−2	1.7E−2	5.9E−4	5.6E−4	1.2E−6	–	1.1E−5
Deactivation constant n_{ij}	0.80				0.99			–	0.45
Case 3 (*product oriented selective catalyst deactivation*)									
Pre-exponential factor $k_{o,ij}$	0.07	0.11	0.00006	3.57	32.04	0.00238	100.25	–	55.11
Activation energy E_{ij}	7.33	9.75	2.92	16.73	15.65	3.79	22.16	–	19.69
Kinetic constant k_{ij} (at 520 °C)	2.3E−1	8.0E−2	3.0E−3	3.1E−2	1.6E−3	2.2E−4	8.0E−5	–	2.1E−4
Deactivation constant n_{ij}	0.83	0.77	0.99	0.61	0.77	0.99	0.61	–	0.61
Case 4 (*reactant oriented selective catalyst deactivation with thermal cracking for dry gas production*)									
Pre-exponential factor $k_{o,ij}$	0.06	0.10	0.00013	3.13	19.65	0.00574	71.71	–	25.63
Activation energy E_{ij}	6.98	9.82	2.30	12.41	16.70	3.87	11.82	–	26.85
Kinetic constant k_{ij} (at 520 °C)	2.6E−1	7.0E−2	1.1E−2	4.2E−1	5.0E−4	4.9E−4	4.0E−2	–	1.1E−6
Deactivation constant n_{ij}	0.82			–	0.98		–	–	–

[a] Pre-exponential factors given in g/gmol s_{ij}^{n-1} for reactions r_{1i} and s_{ij}^{n-1} for all other reactions of Cases 1–3. Their respective units are g/gmol s^{-1} for reaction r_{15} and s^{-1} for reactions r_{25}, r_{35} of Case 4. Activation energies are in kcal/gmol. Kinetic constants are given in wtfrac^{-1} s_{ij}^{n-1} for reactions r_{1i} and s_{ij}^{n-1} for all other reactions of Cases 1–3, for comparison with similar works. Their respective units are wtfrac^{-1} s^{-1} for reaction r_{15}, s^{-1} for reactions r_{25}, r_{35} and s_{ij}^{n-1} for all other reactions of Case 4.

of the parameters of the modified set of Eqs. (1)–(6) for the case of reactant oriented selective deactivation with only thermal cracking considered for dry gas production are shown in Table 4. The relative errors between predicted and experimental yields to each lump are presented in Table 3. In Fig. 6 the relationship between each lump and conversion is presented. This case is analogous to Case 2 with the difference of the hypothesis of thermal cracking for the production of dry gas; therefore Case 4 is straightforwardly compared with Case 2. From this comparison, it is evident that Case 2 and Case 4 have small differences in the prediction of all products except dry gas. Surprisingly, the prediction of dry gas deteriorates, when thermal reactions are assumed for its production. A thorough examination of the plot of dry gas versus conversion in Fig. 6(d) shows that expressing dry gas as a function of gas residence time with no catalyst deactivation dependence, leads to overestimating the effect of feed rate (or gas-oil residence time) on the dry gas production. Moreover, the predicted high values of dry gas yield for low conversions should be examined carefully, but no experimental background exists for this, quite extreme, operational span. Moreover, more realistic results would have been obtained if a small portion of thermal product was considered for all the lumps, but this would have led to increasing the number of unknowns in the regression problem. Finally, if Figs. 4(d), 5(d) and 6(d) are compared to each other, it is evident that Fig. 5(d) (Case 3) stands somewhere in between Figs. 4(d) (Case2) and 6(d) (Case 4). This latter finding can justify a possible coexistence of thermal and catalytic cracking reactions towards dry gas production.

5. Comparison of models—results

The application of the four models to the experimental data of CPERI showed that the differences of the various models are relatively minor. This first impression is in agreement with the many researchers that used non-selective catalyst deactivation in the formulation of their lumping schemes. Corella et al. [28] in a relative work concluded that the difference in the fitting between models with selective and non-selective catalyst deactivation is not very significant, yet they underlined the fact that selective deactivation models are more exact and that they allow for explaining the variation of the distribution of products with time-on-stream. Generally, the results of the three cases that considered only catalytic reactions (Cases 1, 2 and 3) are in good agreement with relative works presented in the literature [29]. The values of the deactivation exponents are relatively higher than those usually reported in the literature [1,20]. This was examined in previous work [19] and was attributed to the design of the CPERI pilot plant, in which relatively higher contact times and larger catalyst inventories occur in the bottom region of the riser. Regarding the rate coefficients obtained in this work, a straight comparison with other values reported in the literature is not always simple, because of the differences in the rate equation formulation of each work. Therefore, it is preferable to compare the product selectivities given by the $k_{1j}/\sum k_{1j}$ ratios. The selectivities calculated by this work and these proposed in the literature are presented in Table 5 and they appear in good agreement to each other, taking into account the differences between the experimental setups and conditions, as well as the different feedstocks and catalysts used by the

Table 5
Selectivity of gas oil to gasoline, gas and coke at 520 °C

Selectivity	Non-selective catalyst deactivation	Reactant oriented selective catalyst deactivation	Product oriented selective catalyst deactivation	Literature values range[a]
$k_{12}/\sum k_{1j}$	0.73	0.72	0.67	0.75–0.80
$(k_{13}+k_{15})/\sum k_{1j}$	0.24	0.25	0.32	0.14–0.16
$k_{14}/\sum k_{1j}$	0.03	0.03	0.01	0.05–0.06

[a] Corella et al. [30], Kraemer and Delasa [31], Lee et al. [3], Ancheyta-Juarez et al. [29].

referred researchers. Nonetheless, a clear conclusion cannot be drawn regarding the selection of the best model of the four cases examined.

An interesting method to explore the possibility of catalyst selective behavior in the fluid catalytic cracking process can be found in the analysis of Ng et al. [21], who examined a simplified version of the four-lump model of Lee et al. [3], by assuming that the gas lump (C_1–C_4) does not produce coke. They used a non-selective catalyst deactivation function of exponential form and after a number of assumptions and mathematical transformations they concluded that for the selectivity of the gas lump and the coke yield Eqs. (7) and (8) should stand:

$$\frac{Y_3+Y_5}{X}=\left(\frac{k_{13}+k_{15}}{\sum k_{1j}}+\frac{k_{12}}{\sum k_{1j}}\frac{k_{23}+k_{25}}{\sum k_{2j}}\right)-\frac{k_{23}+k_{25}}{\sum k_{2j}}\frac{Y_2}{X} \tag{7}$$

$$\frac{Y_4}{X}=\left(\frac{k_{14}}{\sum k_{1j}}+\frac{k_{12}}{\sum k_{1j}}\frac{k_{24}}{\sum k_{2j}}\right)-\frac{k_{24}}{\sum k_{2j}}\frac{Y_2}{X} \tag{8}$$

In Eqs. (7) and (8) the sum $Y_3 + Y_5$ is the total gas yield (LPG and dry gas) in wt%, Y_4 is the coke yield in wt%, Y_2 is the yield to gasoline in wt%, and X is the wt% gas oil conversion. Although, the model of Ng et al. is quite different from the five-lump model described in Eqs. (1)–(5), it still is a significant finding for validating the experimental data and provides a hint to what assumptions are appropriate to each case. The simple translation of Eqs. (7) and (8) is that if the assumptions of non-selective catalyst deactivation and zero gas to coke production hold, then the plots of the selectivity of gas and coke versus the selectivity of gasoline (for constant temperature) should yield straight lines.

In Fig. 7 the plots of gas selectivity versus gasoline selectivity and coke selectivity versus gasoline selectivity are presented. The different data marks correspond to different gas oil feed rates (10, 15 and 18 g/min). Thorough examination of Fig. 7 shows that lower feed rates (higher times-on-stream) yield to lower coke selectivity and higher gas selectivity at the same gasoline selectivity. This observation cannot be ascribed to gasoline secondary reactions yielding to gas and coke for non-selective catalyst deactivation, as the above phenomenon was incorporated in the analysis of Ng et al. [21]. Consequently, one of the two assumptions is not correct: Either the reaction of LPG to coke is significant, or the catalyst deactivation affects in a different manner each reaction. However, it was shown that the reaction of LPG to coke (r_{34}) was found to be negligible for the experimental series examined, which indicates a selective deactivation catalyst behavior in the experiments examined, and can justify the different effect of time-on-stream on the selectivity of coke, gas (LPG plus dry gas) and gasoline. In Fig. 7 the responses of the product oriented selective deactivation model (the model predictions lines) are presented. Case 3 was the case that presented the most significant improvement in the prediction of the selectivity of coke and gas.

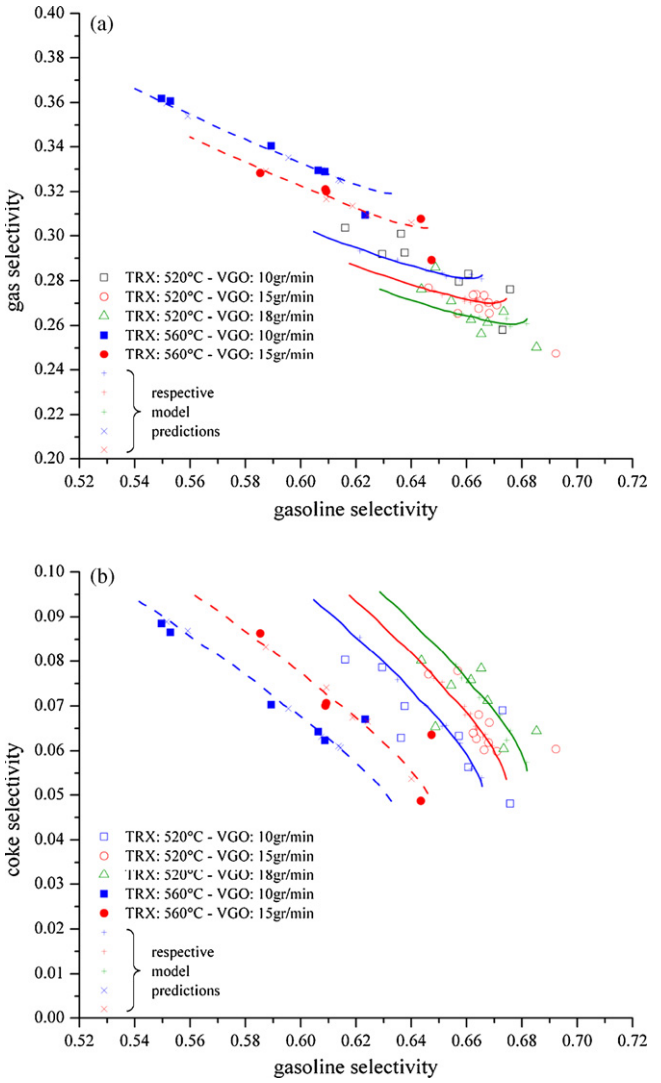

Fig. 7. Product selectivity at different temperatures and feed rates. Symbols present the experimental results and lines present the model predictions: (a) gas selectivity and (b) coke selectivity.

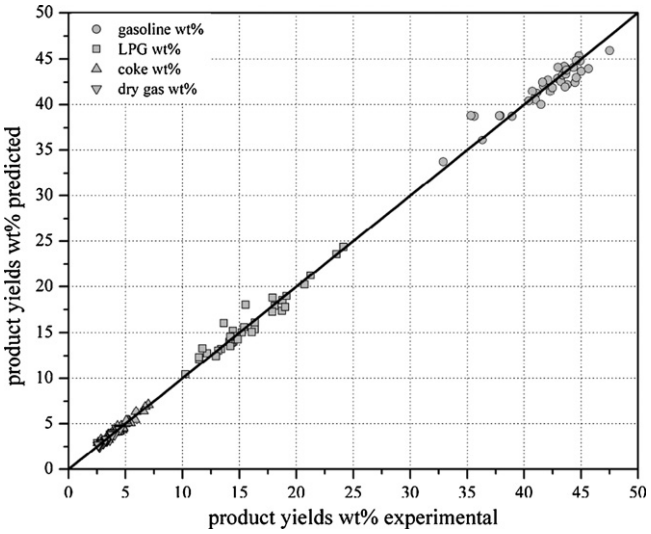

Fig. 8. Predicted vs. experimental yields wt% to each lump for Case 3 (*product oriented selective catalyst deactivation*).

The above analyses showed that better results (quantitatively and qualitatively) can be obtained with the use of a product oriented selective catalyst deactivation function. Fig. 8 presents a typical parity plot of the experimental yields to each product versus the predicted ones, by the product oriented selective deactivation model. The results are satisfactory for all lumps; however, one has to weight the sacrifice in degrees of freedom (model parameters) with the gain in model accuracy (sum of squares). The latter was statistically analyzed with the F-test. Table 6 presents the F-ratios between the cases examined and the respective upper quantiles of Fisher's $\mathcal{F}$ distribution. The only case that succeeds to overcome the performance of the non-selective catalyst deactivation model is the product oriented selective deactivation model, at least from the statistical point of view. A thorough examination of the relative errors of each lump, in the four cases examined (Table 2), reveals that the major improvement of Case 3 is in the prediction of dry gas. The lower catalyst decay exponent for the reactions to dry gas leads to this superiority of the product oriented selective deactivation model. Phenomena as caging, or catalyst sites with different strengths being used for the types of reaction that lead to dry gas can be an explanation to this observation. Another, more engineering and less fundamental, explanation is that the insertion of a discrete deactivation exponent for the reactions yielding to dry gas can bulkily describe the coexistence of catalytic and thermal reactions towards its production. The latter can be attributed by the low value of the decay exponent of dry gas (0.61), which implies a smooth catalyst deactivation profile for the reactions involving dry gas. This smooth profile could be in reality the result of the coexistence of deactivation and non-deactivation effects on the production of dry gas.

Table 6
Statistical comparison of the models examined

Cases compared	F-Ratio	Upper quantile $\mathcal{F}_{0.05}(dF_1 - dF_2, dF_1)$	Winner model
Case 2/Case 1	0.41	3.52	Case 1
Case 3/Case 2	3.72	3.16	Case 3
Case 3/Case 1	9.95	4.41	Case 3

One concern in the development of a reaction network for the fluid catalytic cracker is the applicability of this network to other types of- and to commercial units. It is important to note that the results presented are valid for the experimental database of the pilot plant of CPERI, and much more research has to be performed to advance these findings. However, by the analyses communicated above it is evident that the results of this work are comparable with the results of similar research efforts, which justifies the assumption that both the pilot plant of CPERI and the models presented in this paper are in good agreement with the fluid catalytic cracking reality. As it should be expected by any FCC modeling approach, the proposed models should be applied with caution to other types of FCC units. Nevertheless, one significant outcome of this research effort is that the effect of selective catalyst deactivation should not be neglected, but it should be thoroughly examined when the available experimental data allow for such a study.

6. Conclusions

Four scenarios were examined regarding the way, in which catalyst deactivation should be dealt in lumping models for the simulation of the FCC process in steady state conditions. All models were validated against a database of experiments performed in the FCC pilot plant of Chemical Process Engineering Research Institute at times-on-stream below 18 s. All models comprised of five lumps; gas oil, gasoline, liquefied product gas, coke and dry gas. The investigation of dry gas as a separate lump was proven to be essential, as dry gas does not obey to the same principles with all other catalytic cracking products. The application of the four models showed that the non-selective catalyst deactivation model performs satisfactorily. The only case in which a substantial improvement was made to the model was when a *product oriented* selective catalyst deactivation model was used. This means that the catalyst deactivation effect on the reactions in catalytic cracking is mainly driven or characterized by the products of these reactions. The critical improvement by the use of this model was in the prediction of the yield to dry gas. Phenomena as caging of hydrocarbon molecules in the catalyst pores, or catalyst sites with different acidities being used for different types of reactions, or even the coexistence of thermal and catalytic cracking reactions can justify this finding. In any case, and as Corella and Frances [4], and Wojciechowski and Corma [11] point out in their catalyst deactivation studies, the experimental installation, the experimentation accuracy and the thorough understanding of the significance of each result, are the most important factors in studying the selectivity phenomena during the decaying behavior of FCC catalysts.

Acknowledgements

This work was partially funded by the General Secretariat of Research and Technology Hellas (GSRT) under the program AKMON 110. Helpful discussions with Prof. J. Corella are appreciated.

References

[1] V.W. Weekman, Ind. Eng. Chem. Process Des. Dev. 7 (1968) 90.
[2] L.C. Yen, R.E. Wrench, A.S. Ong, Oil Gas J. 86 (1988) 67.
[3] L.S. Lee, Y.W. Chen, T.N. Huang, W.Y. Pan, Can. J. Chem. Eng. 67 (1989) 615.
[4] J. Corella, E. Frances, in: M.L. Occelli (Ed.), Fluid Catalytic Cracking II (ACS Symposium Series 452), vol. 452, American Chemical Society, Washington, DC, 1991, p. 165.
[5] X. Dupain, E.D. Gamas, R. Madon, C.P. Kelkar, M. Makkee, J.A. Moulijn, Fuel 82 (2003) 1559.
[6] M. Larocca, S. Ng, H. Delasa, Ind. Eng. Chem. Res. 29 (1990) 171.
[7] J. Ancheyta-Juarez, F. Lopez-Isunza, E. Aguilar-Rodriguez, Appl. Catal. A 177 (1999) 227.
[8] T. Takatsuka, s. Sato, Y. Morimoto, H. Hashimoto, Int. Chem. Eng. 27 (1987) 107.
[9] L.L. Oliveira, E.C. Biscaia, Ind. Eng. Chem. Res. 28 (1989) 264.
[10] P. Hagelberg, I. Eilos, J. Hiltunen, K. Lipiainen, V.M. Niemi, J. Aittamaa, A.O.I. Krause, Appl. Catal. A 223 (2002) 73.
[11] B.W. Wojciechowski, A. Corma, Catalytic Cracking, Marcel Dekker Inc., New York, 1986.
[12] S.M. Jacob, B. Gross, S.E. Voltz, V.W. Weekman, AIChE J. 22 (1976) 701.
[13] R.C. Ellis, X. Li, J.B. Riggs, AIChE J. 44 (1998) 2068.
[14] A. Voorhies, Ind. Eng. Chem. 37 (1945) 4.
[15] J. Corella, R. Bilbao, J.A. Molina, A. Artigas, Ind. Eng. Chem. Prod. Res. Dev. 24 (1985) 625.
[16] J. Corella, J.M. Asua, Ind. Eng. Chem. Prod. Res. Dev. 21 (1982) 551.
[17] J. Corella, J.M. Asua, Ind. Eng. Chem. Prod. Res. Dev. 21 (1982) 55.
[18] J. Corella, Ind. Eng. Chem. Res. 43 (2004) 4080.
[19] G.M. Bollas, I.A. Vasalos, A.A. Lappas, D. Iatridis, Ind. Eng. Chem. Res. 41 (2002) 5410.
[20] F.J. Krambeck, in: A.V. Sapre, F.J. Krambeck (Eds.), Mobil Workshop on Chemical Reaction in Complex Mixtures, Van Nostrand Reinhold, New York, 1991, p. 42.
[21] S. Ng, J.S. Wang, Y.X. Zhu, L.G. Zheng, F.C. Ding, L.Y. Yang, S. Yui, Energy Fuels 16 (2002) 593.
[22] G.M. Bollas, I.A. Vasalos, A.A. Lappas, D.K. Iatridis, G.K. Tsioni, Ind. Eng. Chem. Res. 43 (2004) 3270.
[23] IMSL, Fortran Subroutines for Mathematical Applications—Math Library, vol. 1, Visual Numerics Inc., 1997.
[24] Y.T. Shah, G.P. Huling, J.A. Paraskos, J.D. McKinney, Ind. Eng. Chem. Process Des. Dev. 16 (1977) 89.
[25] A.M. Mood, F.A. Graybill, D.C. Boes, Introduction to the Theory of Statistics, McGraw-Hill Higher Ed., London, 1974.
[26] J. Ancheyta-Juarez, J.A. Murillo-Hernandez, Energy Fuels 14 (2000) 373.
[27] J.A. Paraskos, Y.T. Shah, J.D. McKinney, N.L. Carr, Ind. Eng. Chem. Process Des. Dev. 15 (1976) 165.
[28] J. Corella, F.G. Morales, M. Provost, A. Espinosa, J. Serrano, in: Proceedings of the International Conference on Advances in Chemical Engineering (ICACE) Kanpur, India, New Delhi, January 4–6, 1989.
[29] J. Ancheyta-Juarez, F. LopezIsunza, E. AguilarRodriguez, J.C. Moreno-Mayorga, Ind. Eng. Chem. Res. 36 (1997) 5170.
[30] J. Corella, A. Fernandez, J.M. Vidal, Ind. Eng. Chem. Prod. Res. Dev. 25 (1986) 554.
[31] D.W. Kraemer, H.I. Delasa, Ind. Eng. Chem. Res. 27 (1988) 2002.